Pedestrian Indoor Navigation by aiding a Foot-mounted IMU with RFID Signal Strength Measurements

Antonio R. Jiménez Ruiz, Fernando Seco Granja, J. Carlos Prieto Honorato and Jorge I. Guevara Rosas
CAR (Centre of Automation and Robotics). CSIC-UPM.
Ctra. Campo Real km 0.2, 28500 La Poveda, Arganda del Rey, Madrid, Spain.
Email: antonio.jimenez@car.upm-csic.es
Web: http://www.iai.csic.es/lopsi

***Abstract*—We present a methodology to accurately locate persons indoors by fusing Inertial Navigation (INS) techniques with active RFID technology. A foot-mounted IMU aided by the Received Signal Strengths (RSS) obtained from several active RFID tags, placed at known locations in a building, has been used. Other authors have already integrated IMUs with RFID tags in loosely-coupled Kalman Filter (KF) solutions [1], [2], [3]. They feed the KF with the residuals of inertial- and RFID-calculated positions; these approaches do not exploit the benefits of Zero Velocity Updates (ZUPT). In this paper, we present a tight KF-based INS/RFID integration using the residual between the INS-predicted range-to-tag, and the range derived from a generic RSS path-loss model. Our approach also includes ZUPTs at detected foot stances, ZARU (Zero Angular-rate Update) estimation at still phases, and heading drift reduction using magnetometers. A 15-element error state Extended KF [4], [7] compensates position, velocity and attitude errors of the INS solution, as well as IMU biases. This methodology is valid for any kind of motion (forward, lateral or backwards walk, at different speeds) and does not require an specific off-line calibration, neither for the user gait, nor for the location-dependent RSS fading in the building. The integrated INS+RFID methodology eliminates the typical drift of IMU-alone solutions (approximately 1% of the total travelled distance), accounting for typical positioning errors along the walking path (no matter its length) of approximately 1.5 meters.**

I. INTRODUCTION

As GPS is essential for outdoor navigation, there is also a growing need for accurate and continuous indoor localization. Consequently, this topic has received a significant scientific research attention during the last years. There are several location-aware application fields that can benefit from indoor localization, for example: intelligent spaces, personal or asset tracking, guidance of persons with mobility problems, or first-responders for rescue teams or emergencies.

Two main research approaches are used in the indoor positioning problem: 1) Solutions that rely on the existence of a network of receievers or emitters placed at known locations (beacon-based solutions), and 2) Solutions that mainly rely on dead-reckoning methods with sensors installed on the person or object to locate (beacon-free solutions). The first-type beacon-based approaches can use different technologies for the estimation of range or angle between the mobile object and the beacons; it is typical to use ultrasound, radio (WiFi, UWB, RFID, Zigbee, etc.) or vision-based technologies [8]. These beacon-based solutions are normally termed as Local Positioning Systems (LPS). The second beacon-free approaches are sometimes preferable since they do not depend on a pre-installed infrastructure. During the last decade several beacon-free methodologies based on inertial sensors have been proposed for person's location [4], [7], [9]. These methodologies, often called Pedestrian Dead-Reckoning (PDR) solutions, integrate step lengths and orientation estimations at each detected step, or alternatively directly integrate accelerometer and gyroscope readings to compute the position and attitude of the moving person.

978-1-4244-5864-6/10$26.00 © IEEE

IMU-based PDR solutions have the inconvenient of accumulating errors that grow proportional to the path length. For this reason, the integration of both IMU-based and beacon-based LPS solutions has a clear benefit for finding a reliable, continuous and accurate indoor positioning solution.

Other authors [1], [2] have already integrated IMUs with RFID tags in loosely-coupled Kalman Filter (KF) solutions. They feed the KF with the residuals between inertial- and RFID-calculated positions. One of the drawbacks of these implementations is that no Zero Velocity Updates (ZUPT) were employed. Additionally, they use a loose integration, whose performance is in general known to be worse than in tight coupling [10]. In this paper, we present a KF-based INS/RFID tight integration method using the residual between the INS-predicted range to tag, and the range derived from a generic RSS path-loss model. Our approach also includes ZUPTs at detected foot stances, Zero Angular Rate Updates (ZARU) at still phases, and heading drift reduction using magnetometers. A 15-element error state Extended KF [4], [7] compensates position, velocity and attitude errors of the INS solution, as well as IMU biases. Our methodology is valid for any kind of motion (forward, lateral, backwards walk, and so on), and it does not require an specific off-line calibration, neither for the user gait, nor for the location-dependent RSS fading in the building.

The paper is organized as follows. The next section, presents the IMU and RFID sensors used for the indoor location tests. Section III presents a model to relate RSS values to tag-to-

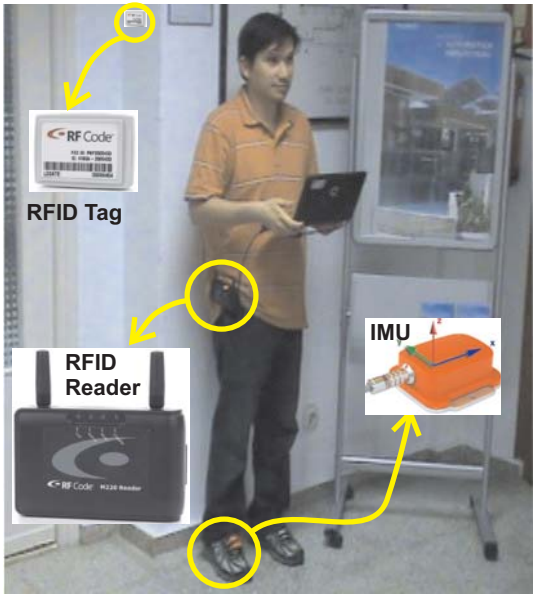

Fig. 1. Sensors used for integrated IMU + RFID navigation. An Xsens IMU is attached to the right foot using the shoe's laces. The RFID reader is on user's waist. Tags are distributed on walls at approximately a 2 m height.

reader distances. Section IV describes the KF-based INS/RFID tight integration method, and finally, section V performs an evaluation of several indoor localization tests. Conclusions are given in last section.

II. IMU and RFID Sensors

A. IMU

We use a commercially available IMU, model MTi from Xsens Technologies B.V (Enschede, The Netherlands; www.xsens.com). Its size is 58 × 58 × 22 mm (Length × Width × Height), and it weights 50 grams. It is configured to provide inertial data at 100 Hz.

The IMU has three orthogonally-oriented accelerometers, three gyroscopes and three magnetometers. The accelerometers and gyroscopes are solid state MEMS with capacitative readout, providing linear acceleration and rate of turn, respectively. Magnetometers use a thin-film magnetoresistive principle to measure the earth magnetic field.

This work uses the IMU mounted on the foot of a person in order to take advantage of Zero Velocity Updates (ZUPT) at foot stances. Fig.1 shows the Xsens sensor fixed to the right foot of a person, using the shoe laces. The exact position and orientation of the IMU on the foot is not important for the algorithms that process the sensor data.

B. RFID

We use active RFID technology from the company RF Code Inc. (Austin, Texas, USA; www.rfcode.com). In our solution we use several tags located at fixed positions within a building, and a portable RFID reader attached to use's waist (Fig. 1).

1) RFID tags: We use active tags model M100, that are battery-powered RF transmitters operating in the 433 MHz radio band. Every tag broadcasts its unique ID and a status message at a periodic rate (1 Hz repetition rate was programmed at the factory). The size of each tag is 46.74 × 34.28 × 11.68 mm (L × W × H). Each tag weights 14.1 grams, including a lithium battery (model CR2032) which is a replaceable coin cell. The expected lifetime is more than 7 years with one emission every 12.5 seconds (according to the manufacturer), so for 1 Hz emission rate the battery lifetime it is expected to be about 6 months. Tags can be put into sleep mode (emissions disabled) using a tag activity controller, model A600 from RFCode; this option is useful to preserve batteries when the system is not to be used during long periods of time.

2) RFID reader: Among the available RF Code readers, we use the model M220 because it is a light-weight portable battery-powered reader. It processes the signals coming from neighboring active RFID tags, and can communicate to a Bluetooth-enabled host processor (PC, PDA, smart phone), and also by a wired USB-serial connection (Bluetooth 1.1 and USB 2.0). The maximum read-out distance between the reader and the tags is up to 70 meters in ideal conditions (free space). The RFID reader is equipped with two short range stub antennas. It is also possible to install 1/4-wave articulated helical antennas for operating at larger distances. Each reader reports the RSS information at each antenna for every in-range tag. The reader size is 111 × 76.5 × 25.1 mm (L × W × H), and it only weights 147 g.

III. RFID acquisition and RSS modeling

A. RSS data acquisition

We have deployed 71 RFID tags in our CAR-CSIC main building (see Fig. 2). The total space inside our building is 2200 m^2. The initial selected tag density is about 1 tag every 30 m^2. This tag density is relatively high, but we decided to use enough tags in order to be able in the future to study the influence of the tag density on the final positioning results.

RSS data-collection experiments were performed by placing the RFID reader at several static positions within the building. The collected RSS data plotted versus the tag-to-reader range (see Fig. 3) clearly shows the typical stochastic nature of RSS measurements caused by multiple fading, reflections, refractions, and multi-paths that are common in complex indoor environments. RSS values, for this specific RFCode reader, ranges from 40 to 110, corresponding a value of 40 to the maximum signal strength, and values approaching 110 for the weakest signals.

The data presented in Fig. 3 corresponds to a total of 32 different reader positions along the main hall and corridor of the CAR-CSIC building. In each position, 1 minute measurements were taken, with 4 different orientations (approximately 15 seconds for each orientation).

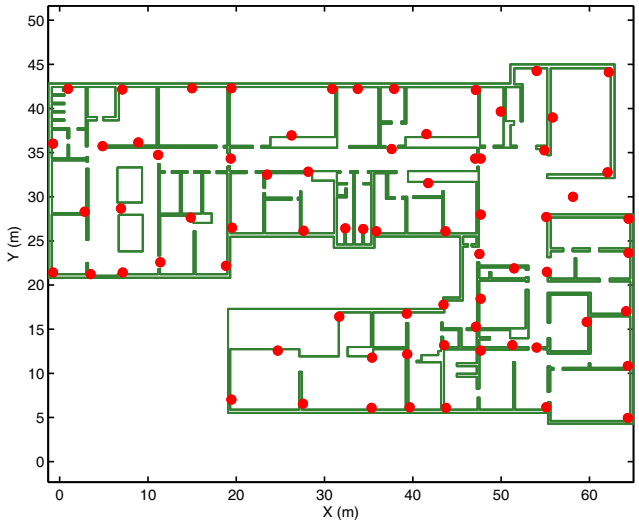

Fig. 2. Distribution of 71 RFID tags (red circles) in our main building.

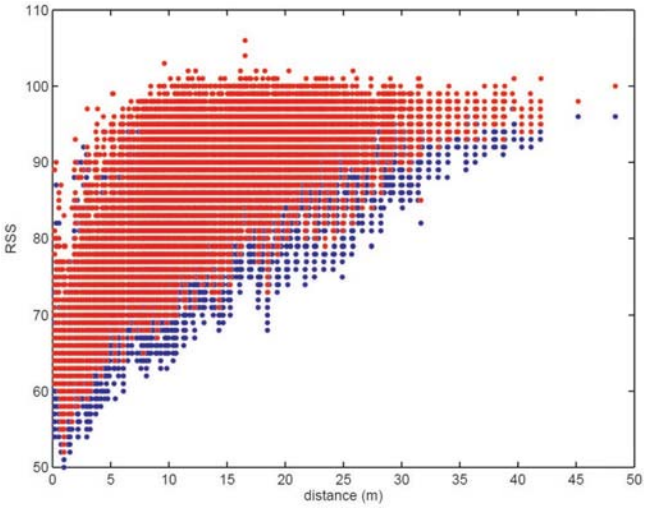

Fig. 3. RSS values versus the tag-to-reader distance. The RSS values captured by both antennas within the reader are coded in different color.

B. RSS-to-distance model

The registered RSS value between the emission of a tag and the reception by a reader, depends on a large number of unpredictable factors (specially indoors). However, there are other factors such as the distance between the emitter and the reader that influence, in a predictable manner, the expected RSS value; this dependency can be used in a RSS model.

The attenuation caused by the distance d between an emitter and a reader, is known as the path loss [5]. This attenuation is inversely proportional to the distance between emitter and receiver raised to an exponent that is know as the path loss exponent p. This exponent p equals 2 for an ideal spherical dispersion in free space, or it can be lower than 2 for propagation along waveguides (e.g. corridors), or larger than 2 when multipath, refraction, or shadowing occurs in the propagation media (typical in buildings). The received power (P_R) at the reader can be modelled as:

$$P_R \propto P_T \cdot \frac{G_t \cdot G_r}{4\pi d^p}, \tag{1}$$

where P_T is the transmitted power at the emitter, G_t and G_r are the antenna gains of transmitter and receiver, respectively, d is the distance between emitter and receiver, and p is the path loss exponent. Using logarithmic units in eq. 1, and considering that RSS is the received power in decibels, we obtain:

$$\text{RSS} = \text{RSS}_0 - 10 \cdot p \cdot \log_{10}\left(\frac{d}{d_0}\right) + v, \tag{2}$$

where RSS_0 is a mean RSS value obtained at a reference distance d_0, and v is a Gaussian random variable with zero mean and standard deviation σ_{RSS} that accounts for the random effect of shadowing [6]. From equation 2 the maximum likelihood estimate of distance d is given by:

$$d = d_0 \cdot 10^{\frac{\text{RSS}_0 - \text{RSS}}{10 \cdot p}}. \tag{3}$$

We obtained the unknown parameters RSS_0 and p, by fitting the experimental data presented in Fig. 3 to the RSS-distance model (eq. 3). We found, for a reference distance d_0 of 1 meter, that RSS_0 equals 60 and p is -2.3 (both parameters have been rounded). The minus sign in the path loss exponent accounts for the inverse dependence of RFCode RSS read-out vs. power (decreasing values of RSS represent stronger signals).

The experimental standard deviation of RSS values, σ_{RSS}, has been found to be an almost distance-independent constant. This value was found to be about 6 RSS units ($\sigma_{\text{RSS}} = 6$). In order to obtain the standard deviation of the estimated distance, σ_d, which is needed by a Kalman filter as an indication of the belief we have on the modelled range value, we use the following heuristic assumption: σ_d must be equal to σ_{RSS} when the slope in model of eq. 3 is 1, and in general it should be reasonably estimated as inversely proportional to the slope of the distance model. If we differentiate eq. 2 with respect to distance d to obtain the slope, we get:

$$\frac{\partial \text{RSS}}{\partial d} = -10 \cdot p \cdot \frac{1}{\ln(10)} \cdot \frac{d_0}{d} \cdot \frac{1}{d_0}, \tag{4}$$

Consequently, the sought standard deviation of distance (σ_d) to be used in our model is:

$$\sigma_d = \sigma_{\text{RSS}} \cdot \frac{\ln(10) \cdot d}{-10 \cdot p}. \tag{5}$$

This sigma model is linearly proportional to distance, so it gives low standard deviation values at short ranges (low uncertainty) and a larger sigma at long ranges (high uncertainty). The combined model representation of RSS versus distance (d and σ_d) is depicted in Fig. 4.

IV. The Integrated IMU+RFID Positioning Method

Before presenting the RFID integration method, we quickly review in the next subsection the basic framework of estimation with an IMU alone, since this framework is the core of the subsequent RFID integration.

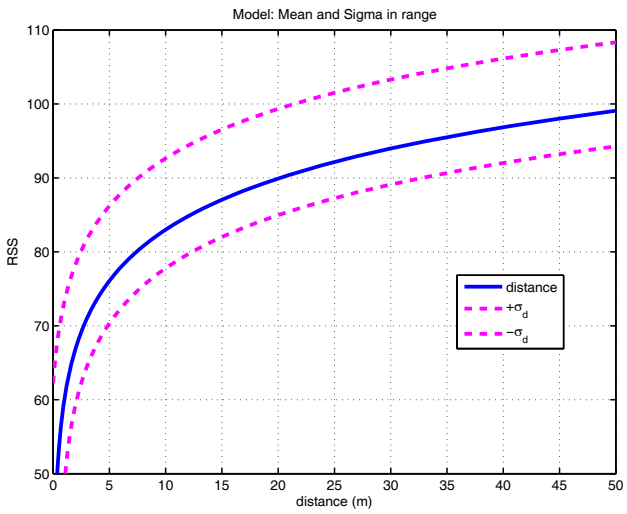

Fig. 4. RSS to distance model. The standard deviation in distance, σ_d (dashed line), is symmetric at both sides of the model plot (solid line).

A. IMU-alone IEZ+ method

The IMU-alone IEZ+ method is a Pedestrian Dead-Reckoning (PDR) positioning method, that was recently presented by Jiménez et al. [7]. This method is an extension of the ZUPT Kalman-based methodology presented by Foxlin [4]. The name of IEZ+ method is a contraction of these acronyms: IMU-EKF-ZUPT-Extended, that stands for "Inertial Measurement Unit - Extended Kalman Filter - Zero Velocity Update - Extended". The reader of this paper is referred to Jiménez et al. [7] for implementation details, nevertheless some key aspects will be highlighted here.

IEZ+ performs an Inertial Navigation (INS) on the foot's position based on IMU readings. This INS process, which is prone to accumulate errors due to IMU biases, is corrected by a 15-element state vector of an Extended Kalman filter (EKF): $\mathbf{X} = [\delta\text{At}, \delta\omega^b, \delta\text{Po}, \delta\text{Ve}, \delta\text{a}^b]$. This vector contains the estimated biases for accelerometers and gyroscopes (δa^b and $\delta\omega^b$, respectively), as well as, the 3D errors in orientation or attitude (δAt), position (δPo), and velocity (δVe).

The EKF is updated (correction phase) with velocity measurements by the ZUPT strategy every time the foot is on the floor. Additionally, the EKF is updated with information about the angular rate of gyroscopes when the foot is still for more than a second (no walking, e.g. standing or sitting). The latter update process is called ZARU, and provides a very good method (fully observable) to quickly find an approximation of gyroscope biases. IEZ+ also incorporates electronic compass information as a quite effective way to limit the drift in heading. Heading errors derived from magnetometer measurements are integrated in the correction/prediction phases of the EKF with the gyro-based error orientation estimations.

The IEZ+ method, using only the self-contained information of the IMU, has proven to be a very reliable PDR method, with accumulated errors of approximately 1% of the total travelled distance [7], [4]. However, over long-distance trajectories this dead-reckoning method can not avoid to progressively diverge from the true path. The integration of external RFID measurements within the IEZ+ (next section) will help to solve this problem.

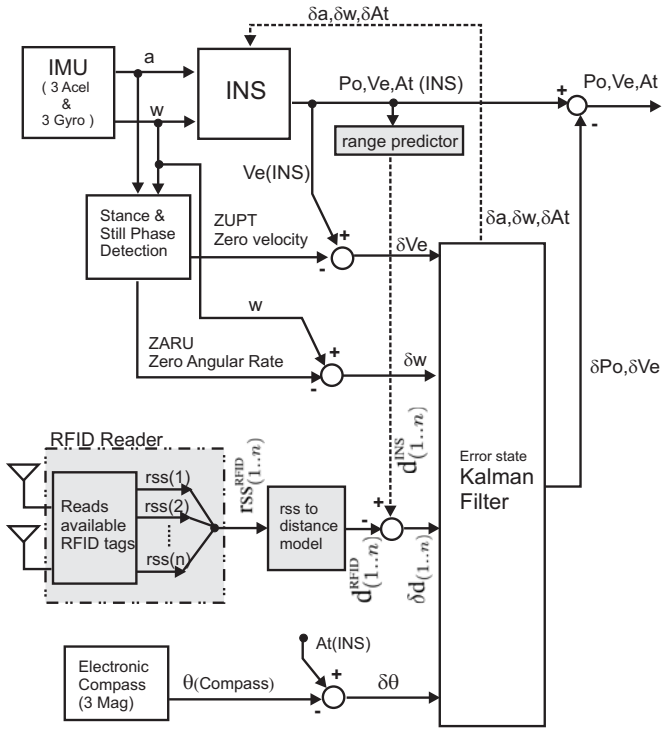

Fig. 5. IEZ+ methodology integrated with RFID measurements for drift-free pedestrian position estimation. Additional blocks for RFID integration are highlighted in gray color.

B. Integration of RFID measurements

We aid the IEZ+ method by means of a tight integration using range residuals estimated from RFID signal strengths. In contrast to other approaches [1], [2], [3] that initially estimate the position using a separate RFID-LPS system and then incorporate positions into the Kalman filter in a loose integration, we use the range-based tight approach which is known to have better performance in GPS and other range-based application areas [10].

The implemented RFID-aided INS indoor pedestrian navigator is depicted in Fig. 5. The whole block diagram corresponds to the IEZ+ methodology that has been complemented, in order to include the RFID information, with three additional blocks: 1) RFID reader, 2) range predictor, and 3) RSS to distance model (blocks in light-gray in Fig.5).

The RFID reader block represents the acquisition phase of RSS values with the M220 RFCode sensor. This RFID data is collected at a 10 Hz update rate. In our implementation we use the average of pairs of RSS values at both antennas, so if n tag emissions are captured at both antennas then n RSS mean values, $\text{RSS}^{\text{RFID}}_{(1..n)}$, are used.

The second additional block in Fig. 5 is a range predictor, which basically provides the tags-to-reader predicted

distances, $\mathrm{d}^{\mathrm{INS}}_{(1..n)}$, i.e. a set of distances between the known positions of detected tags and the current reader (person) position estimated at INS.

The third additional block in Fig. 5 (RSS to distance model) transforms the RSS values into range data using the model in equation 3 as described in last section. The range residual, $\delta\mathrm{d}_{(1..n)} = \mathrm{d}^{\mathrm{INS}}_{(1..n)} - \mathrm{d}^{\mathrm{RFID}}_{(1..n)}$, is fed into the EKF at a 10 Hz rate.

V. Indoor Localization Tests

A. IMU-alone estimation

In this subsection, we analyze the performance of the proposed methodology, but without using the RFID information, i.e. the performance of the IEZ+ method. The IEZ+ method, already presented and assessed in Jiménez et al. paper [7], demonstrated a positioning error of about 1% of the Total Travelled Distance (TTD). The results were very satisfactory, but in that work the paths under evaluation consisted in just one repetition of a given trajectory. Using trajectories where the initial position and the final one were coincident, the total positioning error, was about 1 meter for 100-meter-long trajectories. It is expected, due to the dead-reckoning nature of IEZ+ method, that the final accumulated error will grow by increasing the length of the trajectory, or by repeating several times the same trajectory, even although the percentage with respect to the TTD should remain still about 1%.

Now, we present a set of four indoor tests in our main building, that were repeated several times until the accumulated positioning error was significant (larger than 5 meters). In these tests, we just use a IEZ+ processing, i.e. using the IMU-alone and not the RFID information. However, during these tests we also recorded the sensed RFID data so as to have the opportunity to replicate exactly the same tests in next subsection, but in that case integrating both IMU and RFID data.

The registration of data was performed by a person wearing an IMU on the right foot and an RFID reader on the right side of his waist, both sensors were connected by USB to a netbook computer. The person walks at a normal pace (1 m/s) in forward direction. The doors in the building were opened in order to facilitate the navigation, but the system also works well if the person has to stop to open a door or to wait for another person in his path to pass. Some trajectories include 180 degrees turns when the go and return trajectories coincide.

The four tests together with the estimated trajectories using IEZ+ (IMU-alone) are displayed in Fig. 6. The start position is marked with a black square, and the final position with a black circle and a magenta arrow indicating the direction of the person. The small dots along the trajectory (approximately 1.4 meters apart each other along the path) represents the detected right-foot stances.

As expected, the repetition of the same trajectory several times has finally caused a drift of the position estimation towards an arbitrary direction, and the total error, measured as the distance between the final and initial positions, has grown proportional to the path length or the number of iterations. In Fig. 6a, a 600 meter-long path obtained with 8 repetitions, the error is accumulated at a rate of almost 0.63 meters per cycle, and the start/stop total error is about 5 meters, i.e. 0.8% of total travelled distance. In Fig. 6b, a 550 meter-long path obtained with 13 repetitions, the error is accumulated at a rate of almost 0.77 meters per cycle, and the final error is about 10 meters, i.e. 1.8% of total travelled distance. In Fig. 6c, a 520 meter-long path obtained with 8 repetitions, the error is accumulated at a rate of almost 0.7 meters per cycle and the final error is 7.7 meters, i.e. 1.4% of total travelled distance. Finally, in Fig. 6d, a 1000 meter-long path is obtained repeating 8 times a cycle that includes indoor navigation, and a partial outdoor path along a patio. The error is accumulated at a rate of almost 1.4 meters per cycle, and the total accumulated error is 11.5 meters, i.e. 1.1% of total travelled distance. In these 4 tests the averaged error percentage with respect to the TTD is 1.27%.

B. Integrated IMU+RFID estimation

It is expected that the results obtained in Fig. 6 should be corrected by aiding the IMU-alone processing with an absolute positioning reference given by the RFID equipment. In this section we present the results of the full integrated processing method as presented in section IV. This methodology should limit the total error growth and keep it constant to a value that depends on the maximum accuracy obtainable by an RFID-LPS system (about 2 meters according to most papers in literature [12], [11]), and consequently, the error should not grow with the path length or number of iterations. The same trajectories than in Fig. 6 tests are now displayed in Fig. 7 with the full processing. The position of the installed RFID tags are now displayed on the building maps in Fig. 7 using a red circle.

The presented results are totally satisfactory for pedestrian indoor location. At a first look in Fig. 7, it is clear that the positioning drift is now eliminated when the RFID information is used. The contribution of RFID ranging information, in spite of having a highly stochastic behavior, is incorporated into the final estimation in such a way that the estimated trajectory is as smooth as in the IMU-alone case (Fig. 6). The total error is of 0.8, 2.3, 1.2 and 1 meter, respectively, for Figures 7a, b, c and d. On average, for these 4 tests, the total final error is 1.35 meters (as expected, about 2 meters). The error percentage with respect to the TTD has no sense in this case since it will tend to zero as the path length increases.

VI. Conclusions

In this paper, we have presented a tight KF-based INS/RFID integration method for indoor pedestrian localization and navigation. This method uses the residuals between the INS-predicted range to tag, and the range derived from a generic RSS model. We have shown that the methodology based on a general purpose RSS-to-distance model, does not require a building-specific adaptive calibration for the location-dependent RSS fading in the building. Additionally, since the methodology is based on INS, it does not need any calibration for the user gait (fast/slow, lateral, backwards

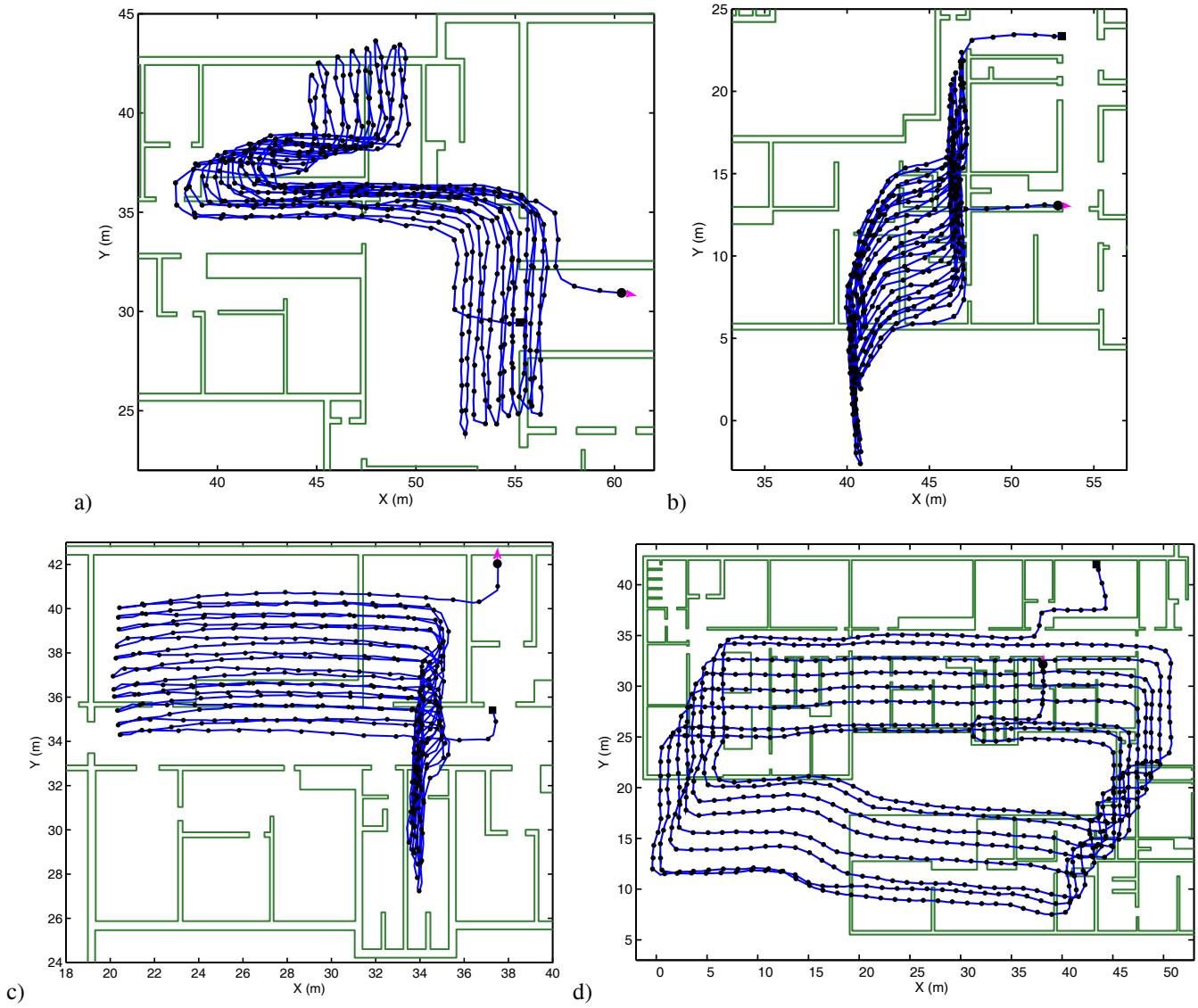

Fig. 6. Different localization tests using the IMU-alone (no RFID information). Several closed cycles are performed along each path (8, 13, 11 and 8 repetitions), with a total length of 600, 550 , 520 and 1000 m, for tests a, b, c, and d, respectively. The total start to stop accumulated errors are 5, 10, 7.7 and 11.5 meters, i.e. in terms of the percentage of the total travelled distance, the error were 0.8% 1.8% 1.4% and 1.1%, respectively.

motion). Pedestrian navigation using only an IMU on the foot, has been shown to slowly drift over long paths or repeated local trajectories. However, our combined integration of INS and RFID information has proven to limit that positioning drift according to the accuracy provided by the network of RFID tags (1 meter for high density of tags, and 3 m for a low density). These results imply that a very accurate pedestrian navigation or guidance is feasible with IMU and RFID technology.

Future work will include the analysis of how the positioning performance is influenced by different settings in the selected RSS-to-distance model parameters, and also how the RFID tag density in the building influences the positioning results. The already attained positioning accuracy is planned to be further improved by integrating the map-building information into the system; in that case, we expect to reach 1 meter accuracy with a very low density of tags.

ACKNOWLEDGMENT

The authors would like to thank the financial support provided by projects LEMUR (TIN2009-14114-C04-03) and LOCA (CSIC-PIE Ref.200450E430).

REFERENCES

[1] V. Renaudin, O. Yalak, P. Tomé, B. Merminod, *Indoor Navigation of Emergency Agents*, European Journal of Navigation, Volume 5, Number 3, July 2007.

[2] K. Zhang, M. Zhu, G. Retscher, F. Wu, W. Cartwright. *Three-Dimension Indoor Positioning Algorithms Using an Integrated RFID/INS System in Multi-storey Buildings*. Lecture Notes in Geoinformation and Cartography, LBS and TeleCartography II, 2009.

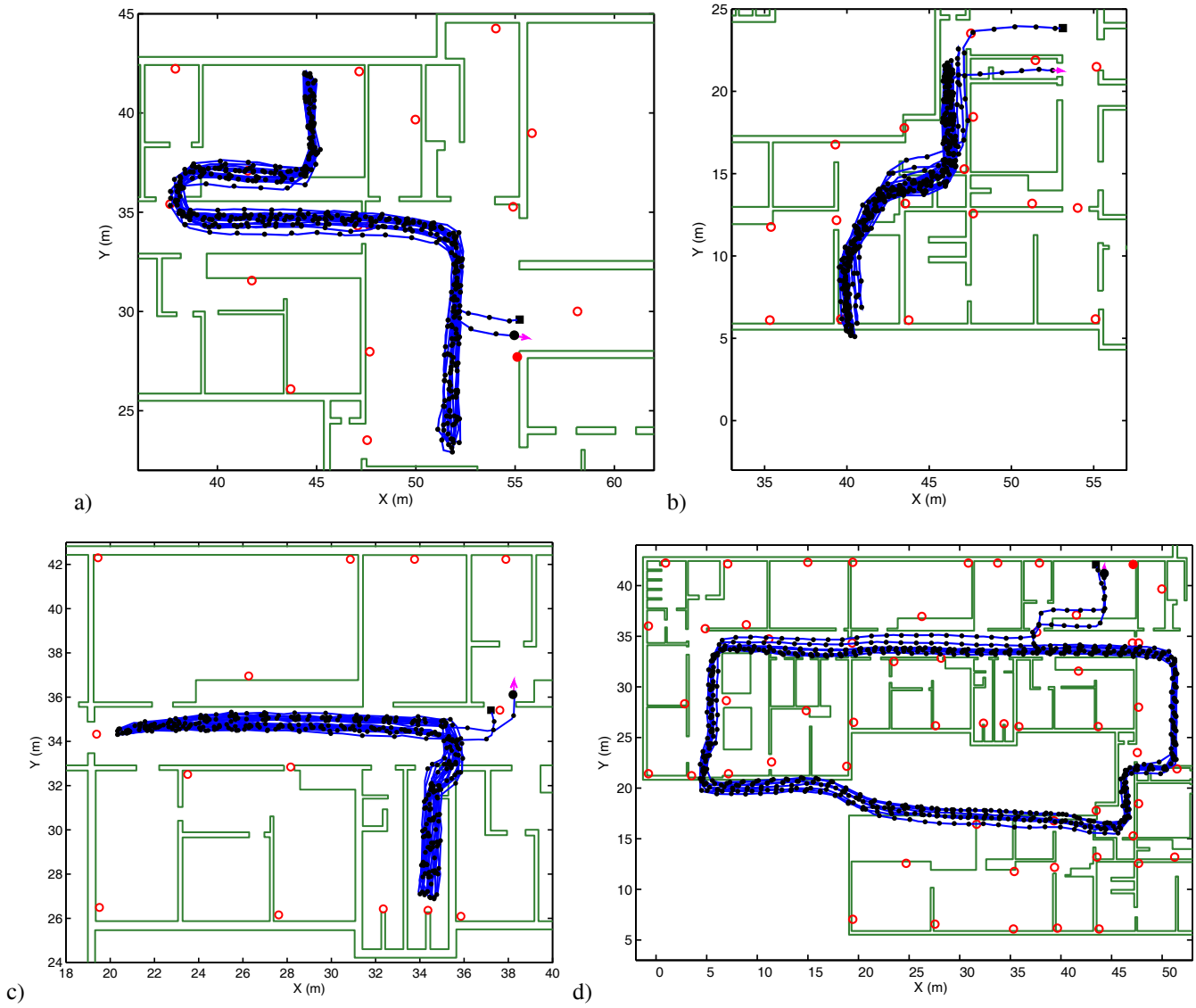

Fig. 7. Position estimation using the proposed integration of RFID to aid the IMU PDR method. The tests are the same of Fig. 6. The error accumulation, as compared to Fig. 6, is strongly attenuated and the start/stop total error is significantly lower: 0.8, 2.3, 1.2 and 1.0 meters, for tests a, b, c, and d, respectively. In terms of a percentage of the total travelled distance, the error were 0.15% 0.45% 0.25% and 0.1%, respectively (Obviously, in the INS+RFID case, it tends to zero as path length increases).

[3] G. Retscher and Q. Fu, *Integration of RFID, GNSS and DR for Ubiquitous Positioning in Pedestrian Navigation*, Journal of Global Positioning Systems, vol.6, No.1: 56-64. 2007.

[4] E. Foxlin, *Pedestrian tracking with shoe-mounted inertial sensors*, IEEE Computer graphics and Applications, vol. 1, pp. 38-46, 2005.

[5] S.Y. Seidel and T.S. Rappaport, *914 MHz Path Loss Prediction Models for Indoor Wireless Communications in Multifloored Buildings*, IEEE Transactions on Antennas and Propagation, 40(2), pp.: 207-217, 1992.

[6] S. Mazuelas, A. Bahillo, R. Lorenzo, P. Fernández, F. Lago, E. Gracía, J. Blas and E. Abril, *Robust Indoor Positioning Provide by Real-time RSSI Values in Unmodified WLAN Networks*, IEEE Journal of Selected Topics in Signal Processing, 3(5), pp.821-831, 2009.

[7] A.R. Jiménez, F. Seco, C. Prieto and J. Guevara, *Indoor Pedestrian Navigation using an INS/EKF framework for Yaw Drift Reduction and a Foot-mounted IMU*, 7th Workshop on Positioning, Navigation and Communication, March 11-12, 2010.

[8] A.R. Jiménez, F. Seco, C. Prieto, and J. Roa, "Tecnologías sensoriales de localización para entornos inteligentes," in *I Congreso español de informática - Simposio de Computación Ubicua e Inteligencia Ambiental, UCAmI2005 (Granada)*, 2005, pp.75-86.

[9] R. Feliz, E. Zalama and J. Gómez, "Pedestrian tracking using inertial sensors," *Journal of Physical Agents*, vol. 3 (1), pp. 35-42, 2009.

[10] Jay A. Farrell and Matthew Barth, "The global positioning system and inertial navigation," *McGraw-Hill*, 1999.

[11] A.D. Koutsou, F. Seco, A.R. Jiménez, J. Roa J. Ealo, C. Prieto, J. Guevara, *Preliminary Localization Results With An RFID Based Indoor Guiding System*, IEEE International Symposium on Intelligent Signal Processing, pp. 917-922, Alcalá de Henares, Spain, October 3-5th, 2007.

[12] F. Seco, C. Plagemann, A.R. Jiménez, W. Burgard, *Improving RFID-Based Indoor Positioning Accuracy Using Gaussian Processes*. International Conference on Indoor Positioning and Indoor Navigation (IPIN), 15-17 September, Zurich, Switzerland, 2010.